Tree Physiology 00, 1–14
doi:10.1093/treephys/tpw126

Research paper

# Dynamics of stem water uptake among isohydric and anisohydric species experiencing a severe drought

Koong Yi[1,5], Danilo Dragoni[2], Richard P. Phillips[3], D. Tyler Roman[4] and Kimberly A. Novick[1]

[1]School of Public and Environmental Affairs, Indiana University Bloomington, 1315 East Tenth Street, Bloomington, IN 47405, USA; [2]Department of Geography, Indiana University Bloomington, 701 East Kirkwood Avenue, Bloomington, IN 47405, USA; [3]Department of Biology, Indiana University Bloomington, 1001 East Third Street, Bloomington, IN 47405, USA; [4]US Department of Agriculture Forest Service, Northern Research Station, 1831 Highway 169 East, Grand Rapids, MN 55744, USA; [5]Corresponding author (koyi@indiana.edu)

Received April 2, 2016; accepted December 22, 2016; handling Editor Nathan Phillips

Predicting the impact of drought on forest ecosystem processes requires an understanding of trees' species-specific responses to drought, especially in the Eastern USA, where species composition is highly dynamic due to historical changes in land use and fire regime. Here, we adapted a framework that classifies trees' water-use strategy along the spectrum of isohydric to anisohydric behavior to determine the responses of three canopy-dominant species to drought. We used a collection of leaf-level gas exchange, tree-level sap flux and stand-level eddy covariance data collected in south-central Indiana from 2011 to 2013, which included an unusually severe drought in the summer of 2012. Our goal was to assess how patterns in the radial profile of sap flux and reliance on hydraulic capacitance differed among species of contrasting water-use strategies. In isohydric species (*Quercus alba* L. and *Quercus rubra* L.), which included sugar maple (*Acer saccharum* Marsh.) and tulip poplar (*Liriodendron tulipifera* L.), we found that the sap flux in the outer xylem experienced dramatic declines during drought, but sap flux at inner xylem was buffered from reductions in water availability. In contrast, for anisohydric oak species, we observed relatively smaller variations in sap flux during drought in both inner and outer xylem, and higher nighttime refilling when compared with isohydric species. This reliance on nocturnal refilling, which occurred coincident with a decoupling between leaf- and tree-level water-use dynamics, suggests that anisohydric species may benefit from a reliance on hydraulic capacitance to mitigate the risk of hydraulic failure associated with maintaining high transpiration rates during drought. In the case of both isohydric and anisohydric species, our work demonstrates that failure to account for shifts in the radial profile of sap flux during drought could introduce substantial bias in estimates of tree water use during both drought and non-drought periods.

*Keywords*: anisohydric, drought, hydraulic capacitance, isohydric, sap flux, stomatal conductance, water regulation.

## Introduction

Drought is projected to occur more frequently and intensely in the coming decades owing to climate change (Nepstad et al. 2002, Schär et al. 2004, Salinger 2005, Bréda et al. 2006), with effects on ecosystem carbon (C) and water cycling that are likely to be particularly consequential for forest ecosystems (Bonan 2008). Forests provide numerous ecosystem benefits and services such as wood production (Schwenk et al. 2012, Verkerk et al. 2015) and regulation of local water cycling (Binkley et al. 1999, Neary et al. 2009, Ford et al. 2011), and are large C sinks globally (Baldocchi 2008, Xiao et al. 2011, Bellassen and Luyssaert 2014). Given that droughts reduce the C uptake capacity of forests (Nepstad et al. 2002, Ciais et al. 2005, Meir and Grace 2005, Bréda et al. 2006) and enhance ecosystem vulnerability to disturbance by fire or insects (Goldammer 1999, Nepstad et al. 1999), an improved understanding of how droughts impact C and water cycling is necessary to better predict potential climate change feedbacks (Bonan 2008).

The extent to which droughts affect forest functioning hinges, in large part, on species-specific responses to water stress (Abrams 2003, Wear and Greis 2012, Brzostek et al. 2014).

This is particularly true in areas like the Eastern USA, where species composition is highly dynamic. In this region, fire suppression in the early 20th century (Abrams 2003, Flatley et al. 2013) has led to a decline on the fractional composition of drought-tolerant oaks species in deciduous forests, thereby increasing vulnerability of the forests to drought events.

An emerging approach is to classify trees' hydraulic strategies along the spectrum of isohydric to anisohydric based on the leaf-level regulation of stomatal conductance (Choat et al. 2012, Manzoni et al. 2013, Klein 2014, Martínez-Vilalta et al. 2014). Trees of higher isohydricity tend to regulate water potential within a narrow range, and thereby reduce the risk of damaging xylem cavitation driven by excessive tension in the trees' hydraulic system (Tyree and Sperry 1988, Choat et al. 2012, Manzoni et al. 2013). The cost of this strategy is that trees close their stomata, which reduces C uptake. Trees inclined to anisohydric behavior, in contrast, tend to allow water potential to decrease during drought. This strategy permits trees to keep their stomata open and maintain C assimilation rates, but with a higher risk of hydraulic failure (Tyree and Sperry 1988, McDowell et al. 2008, Martínez-Vilalta et al. 2014). While the framework of isohydric–anisohydric spectrum has proven useful for understanding tree species' sensitivities to water stress (McDowell et al. 2008, Klein 2014), applying the framework to forests has been more challenging, as leaf-level gas exchange measurements are difficult to scale to the whole canopy (Roman et al. 2015). One possible work-around is to find proxies for leaf-level gas exchange that can be measured relatively easily and at a high temporal frequency.

Sap flux measurements permit continuous observations of tree water uptake at relatively little cost (Swanson and Whitfield 1981, Granier 1987, Hatton et al. 1990, Burgess et al. 2001, Green et al. 2003, Steppe et al. 2010). Dynamics of stem water uptake are often assumed to be linked to the dynamics of transpiration (Oren et al. 1999), though the two fluxes may be decoupled if a tree relies significantly on capacitive discharge of stored water to stabilize physiological function during the day (Meinzer et al. 2009, Scholz et al. 2011, Novick et al. 2015). A defining feature of capacitive sap flux is a reliance on the nocturnal movement of water to refill internal water stores that were depleted during the previous day (Caspari et al. 1993, Daley and Phillips 2006, Wang et al. 2012, Meinzer et al. 2013, Novick et al. 2015). The magnitude of hydraulic capacitance is a critical consideration in the context of drought, as the capacitive discharge of stored water into the xylem conduits in response to increased xylem tension can reduce the risk of hydraulic failure in some species (Meinzer et al. 2009, Scholz et al. 2011, McCulloh et al. 2014). The magnitude of hydraulic capacitance is known to be strongly related to wood traits and soil water availability (which determine the rate of refilling of stored water; Köcher et al. 2013, Oliva Carrasco et al. 2015), as well as to vapor pressure deficit, which is an important driver of stomatal conductance (and thereby determines the withdrawal rate of stored water; Verbeeck et al. 2007). However, whether capacitance is more strongly associated with isohydric and/or anisohydric water-use strategies is relatively unknown (Novick et al. 2016). It is also important to note that while the anisohydric species considered in this study (i.e., the oaks) were also ring-porous, it is not the case that ring-porous species always demonstrate anisohydric tendencies (Martínez-Vilalta et al. 2014).

Linking stem water flux to transpiration rate also requires an estimation of volumetric sap flux over the sapwood conducting area. Often, sap flux observations are made at a single depth in the sapwood and scaled to the whole tree based on the sapwood area (Wullschleger and King 2000, Fiora and Cescatti 2006, Van de Wal et al. 2015). In many cases, however, the rate of sap flux through the stem varies with depth (Phillips et al. 1996, Ford et al. 2004*a*, 2004*b*, Caylor and Dragoni 2009, Dragoni et al. 2009, Van de Wal et al. 2015), and thus estimates of whole-stem water use based only on a single point measurement can be biased. Furthermore, the hydraulic conductivity of sapwood, which may vary with depth into the sapwood, is known to significantly vary among species as well as individual trees (Cermak and Nadezhdina 1998, Wullschleger et al. 1998, James et al. 2002, Köcher et al. 2013, Matheny et al. 2015), making it difficult to understand the water dynamics of forests composed of multiple tree species. For these reasons, radial profiles of sap flux are critical for accurately estimating how whole-tree water use responds to environmental drivers such as droughts, and when applied across multiple tree species and growing seasons, can facilitate up-scaling of point measurements to the ecosystem scale (Phillips et al. 1996, Cermak and Nadezhdina 1998, Nadezhdina et al. 2002, Ford et al. 2004*a*, 2004*b*, Caylor and Dragoni 2009, Dragoni et al. 2009, Shinohara et al. 2013).

Our goal here was to assess how patterns in the radial profile of sap flux and reliance on hydraulic capacitance differed among species that employ contrasting water-use strategies. Specifically, we consider the dynamics of sap flux in two diffuse-porous deciduous hardwood species (*Liriodendron tulipifera* L. and *Acer saccharum* Marsh.) and two ring-porous deciduous hardwood species (*Quercus alba* L. and *Quercus rubra* L.). Tulip poplar (*L. tulipifera*) and sugar maple (*A. saccharum*) were observed to have strong inclination to isohydricity, while white (*Q. alba*) and red oaks (*Q. rubra*) showed strict anisohydric behaviors in a previous study (Roman et al. 2015). Therefore, we categorize tulip poplar and sugar maple as isohydric trees and both oaks as anisohydric trees henceforth, although this isohydric–anisohydric spectrum should not be considered as binary categories, as there are certainly degrees of isohydricity (Franks et al. 2007, Domec and Johnson 2012, Martínez-Vilalta et al. 2014). We hypothesized that the radial profile of sap flux would shift towards the inner xylem during drought (Hypothesis 1), reflecting the action of two mechanisms. First, greater water potential gradient during periods of high transpiration would

exert enough tension to pull the water from the inner sapwood, which typically has a lower hydraulic conductivity (Ford et al. 2004*a*, Matheny et al. 2015). Second, larger water transferring conduits near the cambium may conduct less water during drought if they experience damage from cavitation. We also hypothesized that anisohydric trees that experience relatively low leaf water potentials will rely more on nighttime refilling than isohydric trees, as a mechanism to mediate the effect of large xylem pressure drop under water stress and thereby preventing the risk of xylem cavitation (Hypothesis 2). We addressed these hypotheses using a collection of leaf- (i.e., gas exchange measurement), tree- (i.e., sap flux measurement) and stand-level (i.e., eddy covariance measurement) water flux data collected in south-central Indiana from 2011 to 2013, an interval that included a severe drought in the summer of 2012, which was unseen in decades.

## Materials and methods

### Study site

The study site is located inside the footprint of the Morgan-Monroe State Forest (MMSF) Ameriflux tower in south-central Indiana, USA (39° 19′N 86° 25′W). The average elevation is 275 m above sea level. The MMSF is a secondary mixed hardwood composed of sugar maple (*A. saccharum*), tulip poplar (*L. tulipifera*), sassafras (*Sassafras albidum* (Nutt.) Nees) and oaks (*Quercus* spp.), which represent nearly 75% of total basal area (Schmid et al. 2000). Mean age of the trees is 80–90 years, with a mean height of 27 m (Roman et al. 2015). The soil type is Typic Dystrochrepts dominated by the Berks-Weikert complex, defined as well-drained silt-loam (Dragoni et al. 2011).

In 2012, the MMSF experienced an exceptional drought during the growing season, which allowed us to observe the direct effect of severe drought on the physiological response of our study species. That year, the MMSF received only 23 mm of rainfall during the peak of the growing season (June and July), which is less than 10% of the long-term mean rainfall in June and July (242 mm).

### Eddy covariance measurements and edaphic data

The 46 m flux tower has been continuously recording fluxes of carbon dioxide ($CO_2$), water and energy over the surrounding deciduous forest since 1998 using a 3D sonic anemometer (CSAT-3; Campbell Scientific, Logan, UT, USA) and a closed-path infrared gas analyzer (LI-7000; LI-COR, Lincoln, NE, USA). The data were recorded at a frequency of 10 Hz. Post-processing algorithms include spike detection and removal, correction for the time lag between gas concentration and vertical wind velocity, and a 2D rotation to hourly streamline coordinates (Dragoni et al. 2011). Mean hourly fluxes were computed after excluding the data with net ecosystem exchange (NEE) over ±50 μmol $m^{-2}$ $s^{-1}$ and friction velocity under 0.3 m $s^{-1}$ (Roman et al. 2015).

Climate conditions were classified into drought and non-drought conditions; drought conditions were defined as those occurring when soil water potential ($\Psi_S$) was less than or equal to −0.5 MPa. Non-drought conditions were those occurring when $\Psi_S$ was greater than −0.5 MPa. This critical value is consistent with that chosen by Roman et al. (2015), whose research was also performed at MMSF, and the value represents the minimum weekly mean value of $\Psi_S$ for an average year (defined as mean from 1999 to 2010) at the MMSF site. $\Psi_S$ was calculated as follows:

$$\Psi_S = -2.61 \cdot 10^8 \cdot 189^{-2.51 \cdot (S_w \cdot 100)^{0.14}} \quad (1)$$

where $S_w$ is soil water content ($m^3$ $m^{-3}$), following the approach of Wayson et al. (2006), who used laboratory dry-down experiments to derive the relationship between $S_w$ and $\Psi_S$ for MMSF soils. The $S_w$ in the first 30 cm of the soil was monitored at four different locations in the footprint of the flux tower using time domain reflectometer probes (TDR) (CS615 and CS616; Campbell Scientific). The data was then scaled using gravimetric soil samples collected weekly at the locations of TDR monitoring and a site-wide average $S_w$ was calculated (Roman et al. 2015).

### Sap flux density measurements

Sap flux density was measured for three canopy dominants—sugar maple, tulip poplar and oaks (grouping red and white oaks together)—from 2011 to 2013 using the compensation heat pulse method. Two trees of similar size were measured for each species, and the range of diameters at breast height (DBH) for each species were 41.2–43.8, 62.7–62.8 and 37.5–44.6 cm for sugar maple, tulip poplar and oak species, respectively. Sapwood radii were also determined by visually examining incremental cores from each tree or by using the allometric relationship between DBH and sapwood area proposed by Wullschleger et al. (2001) when visual approach was not suitable. Sapwood radii were 10.9–11.5, 10.2 and 2.0–2.1 cm for sugar maple, tulip poplar and oak species, respectively. We elected to group the oaks together since a preliminary analysis, which was performed to compare red and white oaks, revealed high similarity among these species in terms of the magnitude of sap flux density and its variation over time (data not shown).

The sap flux monitoring system is comprised of a heater, a pair of temperature probes, and a datalogger. The probes and heaters were manufactured specifically for this experiment (Tranzflo NZ LTD, Palmerston North, Manawatu-Wanganui, New Zealand). Each temperature probe has four thermistors inside, which were placed at intervals of 1 cm. This probe design facilitated observations of sap flux density at different depths of sapwood (i.e., 1, 2, 3 and 4 cm away from the cambium in a radial direction). The heater was inserted radially and temperature probes were inserted above and below the heater with an asymmetrical separation distance. The bark of trees was stripped until

bright-colored sapwood was revealed and a hole was made with a drill bit of 2.4 mm diameter. Grease was applied on the probes and heaters to facilitate the insertion and to minimize the gap between the wood and probes/heater. Temperature probes and heaters were connected to a datalogger (CR1000; Campbell Scientific), and the sap flux density was recorded every 15 min. In total, four sets of probes were installed on a single species, with two trees per species and two sets per tree.

The heater probe emits a pulse of heat that warms the water column flowing through the xylem conduit. The warmed portion of the water column acts as a heat pulse and moves upward along the water potential gradient as a tree transpires. Both temperature probes can detect the temperature change caused by heat pulse transfer. Theoretically, the upstream probe (i.e., the temperature probe placed under the heater) detects the heat that was transferred by conduction, and the downstream probe (i.e., the temperature probe placed above the heater) detects the heat transferred by convection and conduction, thereby making it possible to measure the heat pulse velocity with minimized bias related to heat transfer driven by conduction, even during periods of low flow (i.e., nocturnal periods).

The heat pulse velocity ($V$) was calculated using the following equation (Green et al. 2003):

$$V = \frac{X_d + X_u}{2t_z} \quad (2)$$

where $X_d$ is downstream distance from the heater, $X_u$ is upstream distance from the heater and $t_z$ is time delay for the temperatures at points $X_d$ and $X_u$ to become equal. In this study, $X_d$ and $X_u$ were 1.0 and 0.5 cm, respectively.

Convection of the heat pulse is perturbed by the presence of the heater and temperature probes, and by the disruption of xylem tissue associated with their placement. Therefore, the heat pulse velocity should be corrected for the effects of wounding. The correction was performed using the following equation (Green et al. 2003):

$$V_c = 1.184 + 1.072\,V + 0.087\,V^2 \quad (3)$$

where $V_c$ is the corrected heat pulse velocity and $V$ is the raw heat pulse velocity from Eq. (2). The correction coefficients developed for various wound sizes (mm) by Swanson and Whitfield (1981) were used and the wound size was set as 2.4 mm for all trees in this study.

The corrected heat pulse velocity was then converted to the sap flux density ($J_s$) using the following equation (Dragoni et al. 2009):

$$J_s = (0.441 \cdot F_{wood} + F_{water})\,V \quad (4)$$

where $F_{wood}$ is the volume fraction of wood and $F_{water}$ is the volume fraction of water. The volume fractions of wood and water were determined by measuring the fresh weight, dry weight and the volume of wood using incremental cores extracted from each tree.

Data were available for July and August of 2011, 2012 and 2013 for sugar maple and tulip poplar, but only for July and August of 2011 and 2012 in the case of the oaks. In addition to the sap flux measurements, meteorological data were recorded from the flux tower, including air temperature ($T_a$, °C), atmospheric pressure ($P$, kPa), relative humidity (RH, %) and photosynthetically active radiation (PAR, W m$^{-2}$). These data were used in order to calculate canopy stomatal conductance ($g_c$, mmol m$^{-2}$ s$^{-1}$) using a simplified variant of the Penman–Monteith equation:

$$g_c = \frac{E_{ci} \cdot \rho_w \cdot \gamma \cdot \lambda}{\rho_a \cdot c_p \cdot D \cdot \mathrm{LAI}} \quad (5)$$

where $E_{ci}$ is transpiration rate (m s$^{-1}$), which was calculated by scaling $J_s$ up to the tree level by taking averages of $J_s$ at multiple depths of sapwood and then multiplying it by the ratio of sapwood area of each species to stand area, $\rho_w$ is density of water (=1000 kg m$^{-3}$), $\gamma$ is psychrometric constant (kPa K$^{-1}$), $\lambda$ is latent heat of vaporization (J kg$^{-1}$), $\rho_a$ is density of dry air (kg m$^{-3}$), $c_p$ is specific heat capacity (=1006 J kg$^{-1}$ K$^{-1}$), $D$ is vapor pressure deficit (kPa) and LAI is leaf area index. $\lambda$ and $\gamma$ were calculated as follows:

$$\lambda = 2500 - 2.36\,T_a \quad (6)$$

$$\gamma = \frac{c_p\,P}{0.622\,\lambda} \quad (7)$$

In order to convert the $g_c$ from mass unit (m s$^{-1}$) to molar unit (mmol m$^{-2}$ s$^{-1}$), we multiplied Eq. (5) (m s$^{-1}$) by 1000 (1 m = 1000 mm) and then by 40 (1 mm s$^{-1}$ = 40 mmol m$^{-2}$ s$^{-1}$) (Jones 1999). Only the records that were measured under the conditions of $D \geq 1.0$ kPa were used in this study, since the inferred $g_c$ becomes unreliable when $D$ is very low (Oren et al. 1999).

Estimation of transpiration rate based on the sap flux measurement requires a lag-adjustment, because capacitive dynamics of sap flux (i.e., water flux associated with internal water storage) can cause time lags between water fluxes measured in the stem or in the canopy, or between water fluxes measured in the stem and meteorological drivers (Goldstein et al. 1998, Phillips et al. 1999). Therefore, we assessed time lags between stomatal conductance estimated by sap flux and eddy covariance measurements by performing cross-correlation analysis in MATLAB (Mathworks, Natick, MA, USA), using mean hourly data sets of three species for both drought and non-drought conditions. Cross-correlation analysis returns the size of the time lag (number of hours in our case) that lead to the maximum correlation coefficient between a pair of $g_s$ time series estimated from sap flux and eddy covariance measurements (following the approach described in Phillips et al. 1999). The computed time lag for

each species was 1 h for sugar maple and tulip poplar, and 0 h for oaks in both non-drought or drought period. These results were within the range of previously reported time lags between branch and stem base (−8 to +116 min) for five temperate broad-leaved trees (Köcher et al. 2013). We then adjusted the time series of sap flux-based stomatal conductance to remove the time lag between the stem water flow and the micrometeorological drivers.

### *Radial integration approaches of $J_s$*

We compared three approaches for radial profile integration in order to better understand the biases associated with inferring dynamics of stem water uptake in the absence of continuous measurements across the entire sapwood depth. These radial profile approaches are: (i) dynamic integration (DI), (ii) static integration (SI), and (iii) non-integration of radial profile (NI). DI is simply the measured $J_s$ by our sap flux system over the study period; it assumes variable $J_s$ across the sapwood area and $J_s$ also varies with time depending on the environmental conditions. On the other hand, the SI applies a radial integration that does not change over the study period, and is based on averaging hourly $J_s$ during the non-drought period. This integration approach is consistent with some previously published sap flux studies that measured the sap flux across the radial profile for a short period of time, and then use those data to develop a static radial profile integration for all subsequently collected data (Zang et al. 1996, Delzon et al. 2004). The NI approach assumes $J_s$ measured at the single depth of sapwood (average of $J_s$ measured at the sapwood depths of 1 and 2 cm) is representative of the $J_s$ across the entire sapwood area.

### *Gas exchange measurements*

Gas exchange measurements at leaf-level were conducted during the growing seasons of 2011–13, as described in detail in Roman et al. (2015). A boom lift, which could extend up to 24 m, was used to reach the height of canopy and a portable photosynthesis system (LI-6400XT; LI-COR) was used to measure assimilation rates, leaf-level stomatal conductance (hereafter $g_s$) and leaf-level transpiration rate. The measurements were performed every week for three trees per species, and five sunlit canopy leaves were measured for each tree. The environmental conditions inside the leaf chamber (e.g., photosynthetic photon flux density, $CO_2$ and water vapor concentration) were set to match ambient conditions, and each measurement was performed within 2 min in order to avoid the chamber effects. All measurements were averaged for each species and each day, respectively (Roman et al. 2015). The trends in leaf-level $g_s$ values recorded by the portable gas exchange measurement system were compared with the $g_c$ estimated from sap flux measurements. Both data were applied to a diagnostic framework to classify tree water use, as described in the next section.

### *Identifying isohydric/anisohydric behavior*

A diagnostic framework developed by Roman et al. (2015) was adapted to diagnose isohydric and anisohydric behaviors that relates the response of $g_s$ to $D$ as follows:

$$g_s = \frac{1}{D}K(\Psi_S - \Psi_L) = \frac{1}{D}K(\Delta\Psi) \quad (8)$$

where $K$ is the whole-plant hydraulic conductance (mmol $m^{-2}$ $s^{-1}$ $MPa^{-1}$), and $\Psi_S$ and $\Psi_L$ are the soil and leaf water potential, respectively. The contribution of gravitational head losses to $\Delta\Psi$, which is relatively constant over weekly to monthly timescales, was neglected. We use the diagnostic framework to allow the assumption that the relationship between $g_s$ and $D$ would characterize the water use of different species, as $K(\Delta\Psi)$ signifies the species-specific property. Isohydric or anisohydric behaviors were characterized for three species under drought conditions as follows:

- Isohydric behavior: $\Delta\Psi$ decreases during the drought as $\Psi_L$ remains constant, $g_s$ decreases and so does its sensitivity to $D$ relative to the well-watered period.
- Anisohydric behavior: $\Delta\Psi$ remains constant or even increases during the drought as $\Psi_L$ is equivalent to or greater than changes in $\Psi_S$, and $g_s$ and its sensitivity to $D$ are sustained or increased relative to the well-watered period.

It is important to note that this diagnostic framework assumes that $K$ does not change significantly as soil moisture declines. The reasonableness of this assumption for sugar maple, tulip poplar and oak species is discussed in detail in Roman et al. (2015). $K$ was estimated by using transpiration and midday $\Psi_L$ measurements, along with the $\Psi_S$ estimated from pre-dawn $\Psi_L$ measurements. According to Roman et al. (2015), white oak was the only species that showed significant changes in $\Delta K$ ($P = 0.01$) with little decrease over the drought period ($\Delta K = -1.1$ mmol $m^{-2}$ $s^{-1}$ $MPa^{-1}$ over ~70 days, slope = −0.016, $R^2 = 0.91$). Therefore, we concluded that embolism in plant's xylem during the severe drought period was not significant in the case of the trees monitored in this study.

While Eq. (8) predicts that $g_s$ will relate to the inverse of $D$, modifications to $K$ and $\Delta\Psi$ during periods of water stress will decouple the relationship between $g_s$ and $D^{-1}$. In this study, variation in the relationship between $g_s$ and $D$ was expressed using a function that emerges from assumptions of optimal stomatal functioning and that has been shown to agree well with other empirical functional forms (Katul et al. 2009):

$$g_s = a - bD^{-0.5} \quad (9)$$

The linear relationships between $g_s$ and $D^{-0.5}$ established for different measurements and $\Psi_S$ conditions were normalized by dividing all curves by the value of $g_s$ at $D = 1$ kPa. In this way,

trends in the temporal dynamics of $g_s$ may be evaluated across scales.

### *Integration of water-use measurements at different levels*

Hydraulic characteristics of canopy-dominant trees in MMSF were assessed by integrating three different observation levels, namely leaf-, tree- and stand-levels. Leaf-level water use was observed by measuring gas exchange at the canopy using the portable photosynthesis system, tree-level water use was observed by sap flux measurement technique and stand-level water use was observed by the eddy covariance method. More specifically, we tried to find evidence for (i) a reliance on stored water by comparing stomatal conductance at the leaf- ($g_s$) and tree-levels ($g_c$), and for (ii) refilling of stored water by comparing nighttime water flux at tree- and stand-levels.

For the leaf- and tree-level comparison, we assumed that a decoupling between $g_s$ and $g_c$ indicates withdrawal of stored water, assuming that water flux at the leaf-level represents the sum of water flux along the soil–plant–atmosphere continuum and capacitive discharge of stored water into the transpiration stream. This approach is analogous to that used in previous studies of hydraulic capacitance comparing sap flux density measured at trunk- and upper branch-levels (Wullschleger et al. 1998, Phillips et al. 2003).

For the assessment of nighttime water flux, the monthly ratio of nighttime to total daily water flux (N/T ratio) was computed to compare the water flux at tree- and stand-levels. We assumed that a relatively higher contribution of nighttime water flux at the tree-level (compared with the stand-level) represents the refilling of stored water, which was lost by a high demand for transpiration during the day, noting that the stand-level, tower-derived estimates of nocturnal evapotranspiration (ET) cannot detect water movement within the canopy. Here, nighttime was defined as the time period from 9 p.m. to 6 a.m. EST, which corresponded to the hours after sunset and before sunrise during the study period. The impact of drought on the tree's withdrawal and refilling of stored water was also assessed by comparing their responses in drought and non-drought periods.

### *Statistical analyses*

The impact of drought on the species-specific water-use strategy was evaluated by statistically comparing their responses under non-drought and drought conditions. All statistical analyses were performed using MATLAB and SPSS statistical software packages. The $g_s$ response at given $D$ values during non-drought and drought periods was compared for each species using a $t$-test. The effectiveness of multiple radial correction methods was assessed by computing NI/DI and SI/DI, which implies over- or underestimation of DI if the ratio is over or under 1, respectively. The impact of drought on each ratio was compared by performing a $t$-test. Finally, the effect of drought on N/T ratio was compared for each species using a $t$-test. All $t$-tests were performed with 95% confidence intervals.

## Results

NEE and ET observed from the eddy covariance method revealed a significant impact of drought on C and water exchange in MMSF. NEE was reduced by more than 50% during the growing season (DOY 182–218) in 2012 relative to the long-term mean NEE (1999–2013; Figure 1). Likewise, ET was also reduced ~50% during the same period (Figure 1), implying the tight relationship between C and water dynamics. In the following subsections, we turn our attention to the species-specific drought responses.

### *Diurnal pattern of radial profile*

All species shared a common pattern of diurnal sap flux variation, which started to increase around the time of sunrise, peaked at mid-afternoon and dropped gradually until sunset (Figure 2). However, species-specific differences were found in

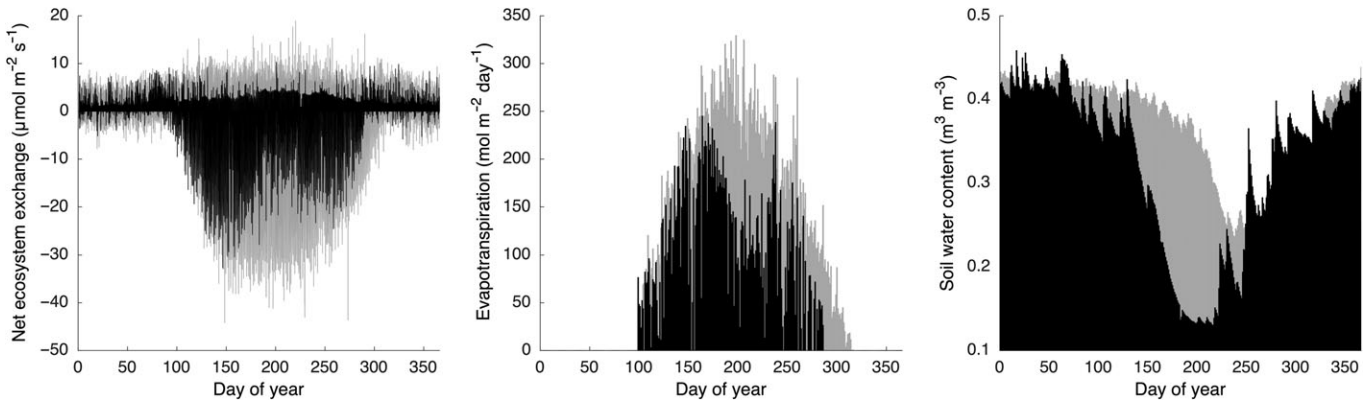


Figure 1. Annual NEE (left), ET (middle) and soil water content (SWC, right) from 1999 to 2013 measured at Morgan-Monroe State Forest located in Bloomington, IN. Black line indicates NEE, ET or SWC observed in 2012 (year of drought) and gray line indicates the composite of NEE, ET or SWC observed from 1999 to 2013 except 2012.

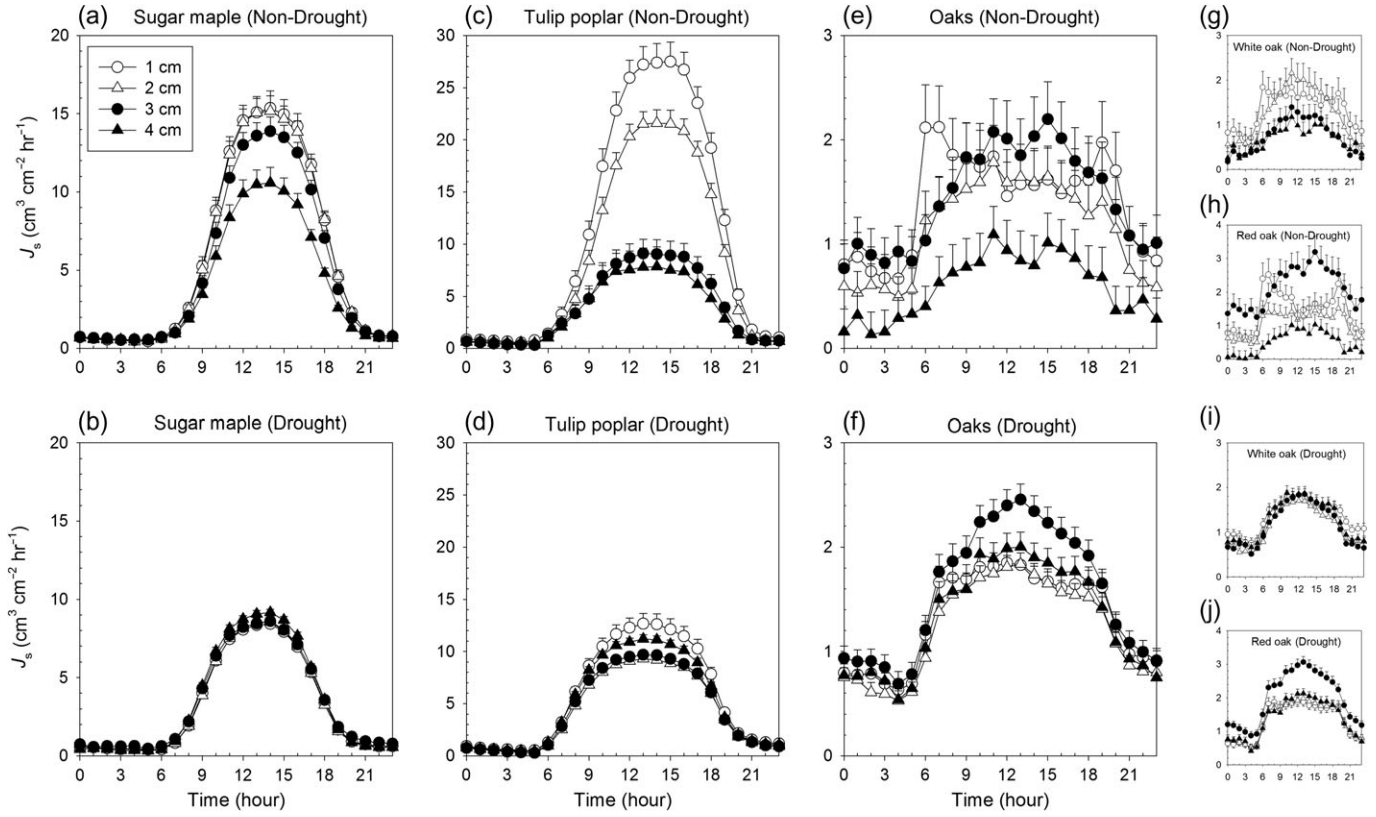


Figure 2. Mean hourly sap flux density ($J_s$) of sugar maple, tulip poplar and oaks measured at the different depths of sapwood (1, 2, 3 and 4 cm away from cambium in radial direction) during the non-drought ($\Psi_S > -0.5$ MPa) and drought ($\Psi_S \leq -0.5$ MPa) periods. Error bars (only positive sides are depicted) represent standard errors of the hourly means (95% confidence).

the magnitude of sap flux variations at a single depth and the pattern of the radial profile under drought and non-drought conditions.

The diurnal pattern of sap flux during the drought period, compared with the non-drought period, was characterized as a relatively large decrease of sap flux in the outer sapwood (i.e., the 1 and 2 cm depths), but a relatively small decrease of sap flux in the inner sapwood (i.e., the 3 and 4 cm depths). As a result, the trees' reliance on water conducted through the inner sapwood was higher during drought. These patterns were pronounced for tulip poplar and sugar maple, but were less clear for the oaks. Decoupling of oaks' sap flux pattern into individual species (white and red oaks) revealed that the irregular diurnal pattern was mainly attributable to the red oak (Figure 2). Unlike the red oak, sap flux in the outer sapwood of white oak was reduced during drought, similar to other species. The difference between the peaks of the diurnal sap flux curves during the non-drought and drought periods was as follows: the net decrease (−) or increase (+) in sap flux (units cm$^3$ cm$^{-2}$ h$^{-1}$) at 1, 2, 3 and 4 cm depths of sapwood during drought were −6.9 (−45%), −6.6 (−44%), −5.3 (−38%) and −1.4 (−14%) for sugar maple, −14.8 (−54%), −12.3 (−57%), +0.6 (+6%) and +3.3 (+43%) for tulip poplar, and −0.3 (−13%), +0.1 (+3%), +0.3 (+12%) and +0.9 (+83%) for oaks, respectively (Figure 2).

The highest sap flux was found during the non-drought period in sugar maple and tulip poplar, with average mid-day rates of 15.4 and 27.5 cm$^3$ cm$^{-2}$ h$^{-1}$, respectively. However, oaks' highest sap flux was found during the drought period (2.5 cm$^3$ cm$^{-2}$ h$^{-1}$) (Figure 2). During the drought period, the net decrease (−) or increase (+) in the highest sap flux (units cm$^3$ cm$^{-2}$ h$^{-1}$) was −9.2 (−40%), −12.7 (−54%) and +0.3 (+12%) for sugar maple, tulip poplar and oaks, respectively, indicating higher sensitivity of sugar maple and tulip poplar to the drought than that of oaks (Figure 2).

### *Radial profile integration of sap flux density*

An estimate of the tree's water use made by assuming the sap flux of the outer sapwood was constant over the radial profile of sapwood (NI) differs significantly from the estimate of the tree's water use made by taking advantage of the radial profile measurements (DI). During the non-drought period, sap flux integrated by NI ($J_{s,NI}$) overestimated sap flux integrated by DI ($J_{s,DI}$) by 42% and 8% for tulip poplar and sugar maple, respectively (Table 1). However, during the drought, $J_{s,NI}$ underestimated $J_{s,DI}$ by 4% and 2% for sugar maple and tulip poplar, respectively (Table 1). Thus, for these species, if sap flux observations in the outer xylem are used to estimate the total stem water use, reductions in water uptake during drought will be overestimated. In

Table 1. Ratio of non-integration of $J_s$ (NI: assumes constant $J_s$ over the range of sapwood area but variable over time) to dynamic integration of $J_s$ (DI: assumes variable hourly $J_s$ over the range of sapwood area, and also variable over study period) and ratio of static integration of $J_s$ (SI: assumes hourly specific $J_s$ for each depth, but invariable over study period) to $J_{s,DI}$. The values are presented as mean ± standard error (95% confidence). Ratios >1 indicate that NI or SI approaches overestimated water flux compared with the estimation made by DI approach. Ratios <1 indicate that NI or SI approaches underestimated water flux compared with the estimation made by DI approach.

| Ratios | Sugar maple | | Tulip poplar | | Oaks | |
|---|---|---|---|---|---|---|
| | Non-drought | Drought | Non-drought | Drought | Non-drought | Drought |
| NI/DI | 1.08 ± 0.01 | 0.96 ± 0.01 | 1.42 ± 0.01 | 0.98 ± 0.01 | 0.95 ± 0.02 | 0.90 ± 0.01 |
| SI/DI | 0.98 ± 0.02 | 0.84 ± 0.01 | 0.99 ± 0.02 | 0.70 ± 0.01 | 1.04 ± 0.02 | 0.27 ± 0.00 |

the case of oaks, $J_{s,NI}$ underestimated $J_{s,DI}$, regardless of water availability (5% and 10% for non-drought and drought conditions, respectively; Table 1).

On the other hand, the difference between sap flux integrated by SI ($J_{s,SI}$) and $J_{s,DI}$ during the non-drought period was not as large as the difference between $J_{s,NI}$ and $J_{s,DI}$, showing only 2% and 1% underestimation for sugar maple and tulip poplar, respectively, and 4% overestimation for oaks (Table 1). However, the difference between $J_{s,SI}$ and $J_{s,DI}$ was larger than the difference between $J_{s,NI}$ and $J_{s,DI}$ during the drought period, showing 16%, 30% and 73% underestimations for sugar maple, tulip poplar and oaks, respectively (Table 1). Thus, integrating sap flux data collected in the outer xylem during drought with a radial profile measured during non-drought conditions would also tend to overestimate the extent to which drought conditions reduce tree water use.

### *Stomatal conductance during the drought period*

Decreasing $g_s$ and $g_c$ with $D$ were observed for all species, although their responses to the drought were not identical. The shifting patterns of $g_c$–$D$ curves observed from the sap flux measurement from the non-drought to drought period were consistent with the patterns observed from the gas exchange measurements (i.e., $g_s$–$D$ curves; Figure 3), as the decrease in $g_c$ and $g_s$ was more pronounced in both sugar maple and tulip poplar than in oaks during the drought. Vapor pressure deficit ($D$) rarely exceeded 3 kPa during the non-drought period but reached up to 5.1 kPa during the drought period. For tulip poplar, $g_c$ during the drought period was significantly lower than the non-drought period when $D$ was between 2 and 3 kPa ($P < 0.05$), but not when $D$ was lower. The $g_c$ of sugar maple and oaks were not significantly different between drought and non-drought periods at any of the $D$ levels ($P > 0.05$), though $g_s$ of oak species was observed to increase at a given $D$ during the drought period (Figure 3). At a given $D$, normalized $g_s$ was higher than the normalized $g_c$ for all species, indicating trees' withdrawal of stored water (Figure 4).

### *Nighttime refilling of water storage*

The ratio of nighttime to total daily water fluxes (N/T ratio) in all three species were higher at the tree-level than the stand-level (Figure 5). However, the degree of reliance on the nighttime refilling varied across the species. The highest N/T ratio was observed for oaks in both non-drought and drought periods, reaching 19.8% and 18.4%, respectively, with no significant difference between the two periods ($P > 0.05$; Figure 5). The N/T ratio for sugar maple and tulip poplar only reached 4.6% and 3.3% during the non-drought period, and 6.6% and 6.3% during the drought period, respectively. Among the species, significant difference between non-drought and drought periods ($P < 0.05$) was observed for sugar maple and tulip poplar (Figure 5).

## Discussion

The species-specific relationship between $g_s$ and $D$ and its shift between drought and non-drought conditions observed in the sap flux measurements confirmed previous results based on gas exchange measurements (Roman et al. 2015). This convergence suggests that sap flow measurement is a useful tool to diagnose water-use strategies of broad-leaf species under water-limiting conditions. In both leaf- and tree-level approaches, sugar maple and tulip poplar showed isohydric behaviors during the drought period with reduced $g_s$ and $g_c$, while oaks maintained high levels of $g_s$ and $g_c$, consistent with anisohydric behavior. Although sugar maple and tulip poplar were both isohydric in general, a range of evidence suggested more active physiological regulation of water use by tulip poplar, including larger differences of sap flux, $g_s$ and nighttime refilling between non-drought and drought periods.

Under the condition of water stress, the magnitude of water flux decreased and the contribution of outer xylem to total water flux declined. This resulted in a shift of the radial profile of sap flux, which was more noticeable in isohydric species than in anisohydric species. Comparison of radial profile integration approaches revealed the importance of taking radial profiles into account when assessing the impact of drought on water flux. Both NI and SI approaches substantially over- or underestimated water flux compared with DI, implying that disregarding the radial profile entirely (i.e., the NI approach; see Clearwater et al. (1999) and Nadezhdina et al. (2002)) or failing to account for how it shifts with varying drought conditions (i.e., the SI approach; see Fiora and Cescatti (2006) and Nadezhdina et al. (2007)) would

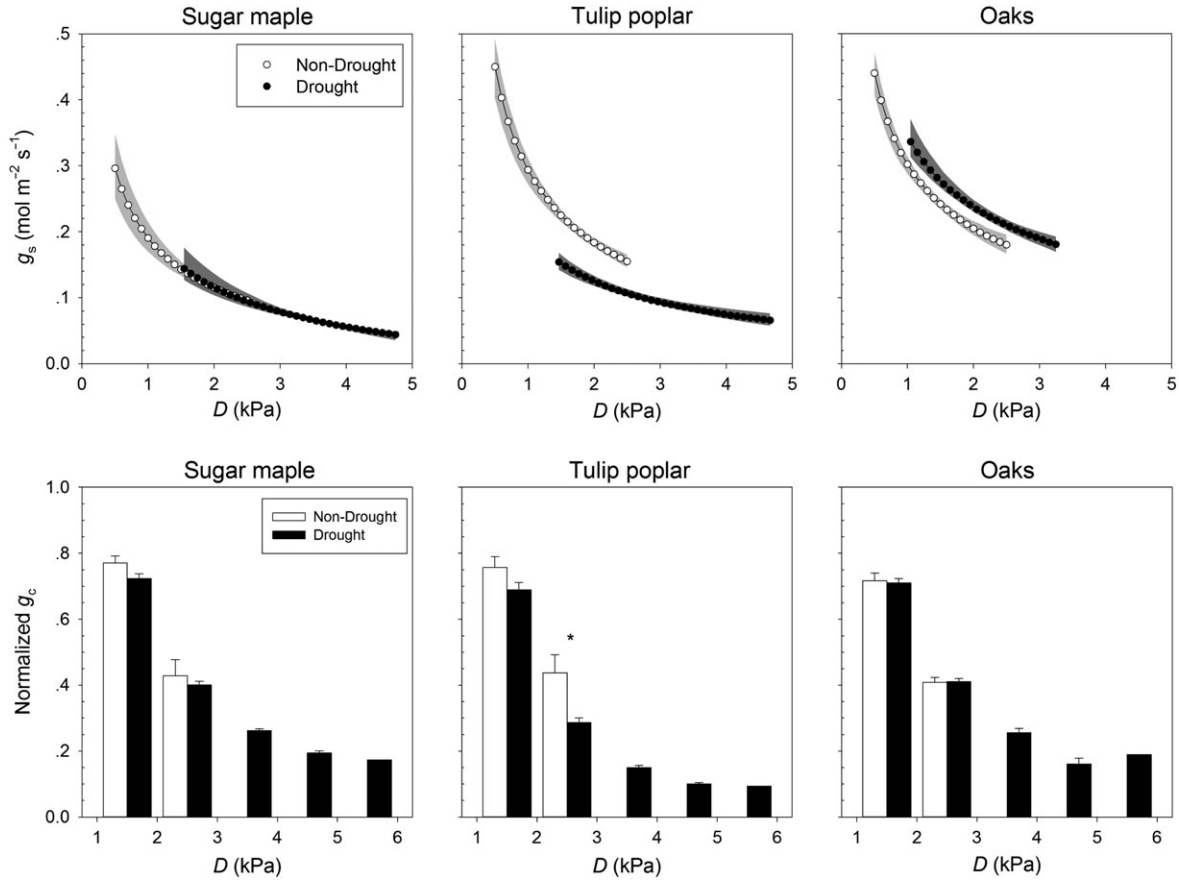


Figure 3. The relationship between $g_s$ and $D$, observed by gas exchange measurement (top, the figure is originally from Roman et al. (2015)) and between normalized $g_c$ and $D$, by sap flux measurement (bottom). Open and closed circles represent $g_s$ during non-drought and drought period, respectively. Light and dark gray areas in the top figures indicate 90% confidence intervals of non-drought and drought periods, respectively. Error bars represent standard errors of the means (95% confidence). Asterisks above the bars represent significant differences between non-drought and drought periods ($P < 0.05$).

potentially overestimate the impact of drought on the reduction in water uptake. We also found evidence of discharge of stored water in trees from the observation of higher $g_s$ compared with $g_c$, and nighttime refilling of water storage by comparing the ratio of nocturnal to total water flux at the stand- and tree-levels. Hydraulic capacitance was inferred to be especially important for oak species, indicating their ability to mediate the risk of hydraulic failure and to maintain their C uptake rate despite the high demand of transpiration during drought.

### *Hydraulic capacitance*

In this study, the ratio of nocturnal to total daily water use was considerably higher at the tree-level than at the stand-level (Figure 5), suggesting that the nocturnal sap flux primarily reflected refilling of stored water in both drought and non-drought conditions. Previous studies have also reported the trees' stomata opening at night, which would allow both night-time transpiration and refilling of stored water (Daley and Phillips 2006, Fisher et al. 2007, Novick et al. 2009, Wang et al. 2012). According to our results, however, nocturnal ET remained low relative to the water uptake estimated by sap flux measurements (Figure 5). Therefore, we presume that, at least in our case, the nocturnal transpiration was not likely the predominant mechanism driving nocturnal water uptake but the refilling of stored water. The rooting depth of oaks, which is often found to be deeper compared with other tree species (Abrams 1990), might allow access to deep soil water, and higher soil water availability might aid them in refilling stored water (Köcher et al. 2013, Thomsen et al. 2013). Nonetheless, $\Psi_S$ estimated from pre-dawn $\Psi_L$ measurements in our study revealed relatively lower $\Psi_S$ for oaks than sugar maple and tulip poplar (see Roman et al. 2015), suggesting less soil water availability for oaks. Therefore, the difference in N/T ratios among species in our case is less dependent on soil water availability but rather related to species-specific characteristics.

The marginal difference in the N/T ratio by oak species between drought and non-drought periods is likely linked to the fact that sap flux is overall less variable between the two periods. Although the isohydric species' reliance on nighttime refilling might not be as large as the anisohydric species, this behavior

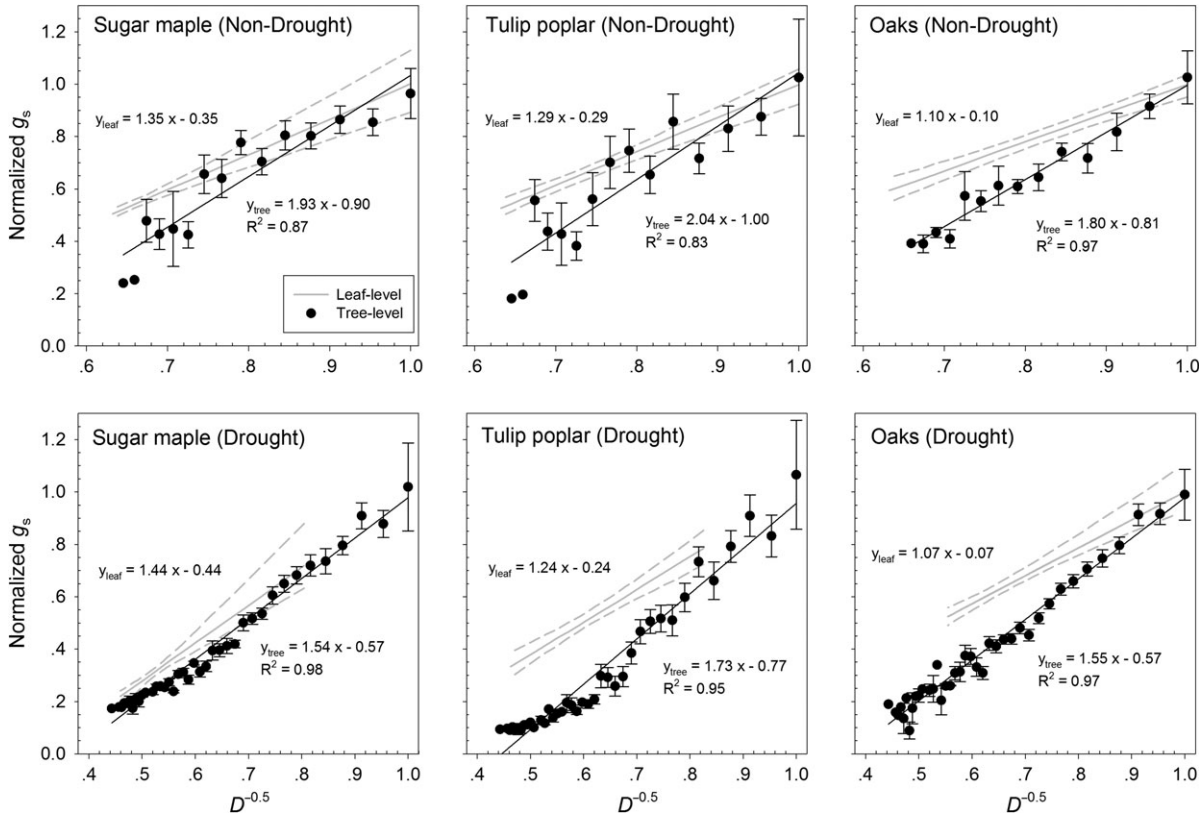


Figure 4. The relationship between $g_s$ and $D^{-0.5}$, observed by gas exchange measurement (leaf-level, data originally from Roman et al. (2015)) and sap flux measurement (tree-level). Black and gray solid lines indicate linear regression of sap flux and gas exchange measurements, respectively. Broken gray lines indicate 90% confidence intervals of gas exchange measurements.

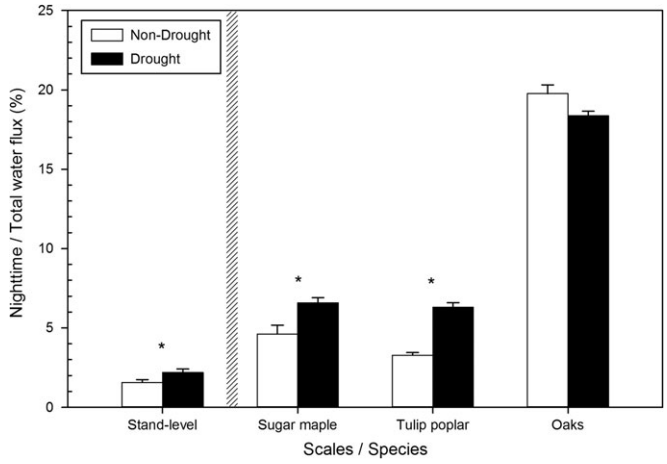


Figure 5. Ratio of nighttime to daily total water fluxes (N/T ratio) estimated at stand- and tree-levels. The stand-level water flux was estimated by flux tower measurements, and the tree-level water flux was estimated by sap flux measurements. Error bars represent standard errors of the ratio means (95% confidence). Asterisks above the bars represent significant differences between non-drought and drought periods ($P < 0.05$).

along with the shift of radial sap flux profile would still play a crucial role in mediating reduced transpiration during the period of water limitation. Therefore, our results suggest that failing to properly measure nocturnal sap flux would result in a biased role of nighttime refilling in mediating the risk of hydraulic failure (Figure 5). Despite the variety of available sap flux measurement techniques (e.g., thermal dissipation, heat pulse velocity, and heat field deformation methods) and their ability to measure nighttime sap flux (Green et al. 2003, Ford et al. 2004*a*, Daley and Phillips 2006, Fisher et al. 2007, Oishi et al. 2008), inadequate data processing (e.g., failure to assume zero-flow conditions correctly or setting wrong baseline for nighttime flux) may lead to incorrect measurements of nighttime sap flux (Steppe et al. 2010). Furthermore, determining the extent of hydraulic capacitance is challenging in some studies due to the fact that some sap flux methodologies do not adequately account for nocturnal flow rates (Regalado and Ritter 2007). Thus, care should be taken in determining nighttime sap flux, and understanding characteristics and limitations of each sap flux measurement technique is critical to process nighttime sap flux data properly.

The evidence of stored water usage is further supported by a decoupling between leaf- and tree-level relationships between stomatal conductance and $D$ (Figure 4). The leaf-level $g_s$ was less sensitive to $D$ than the tree-level $g_c$, suggesting the capacitive discharge of stored water into xylem, which dampens the fluctuation of water flux caused by abrupt changes in xylem tension and consequently reduces the risk of xylem embolism and hydraulic failure (Phillips et al. 2003, Scholz et al. 2011,

Matheny et al. 2015). Withdrawal of stored water in the stem, which was inferred from the difference in the slope between stomatal conductance estimated by leaf- and stem-level over $D^{-0.5}$ (Figure 4), revealed that sugar maple decreased the withdrawal during the drought period (i.e., smaller difference between leaf- and stem-level $g_s$ slopes during drought), while tulip poplar and oaks slightly increased the withdrawal during drought period (i.e., larger difference between leaf- and stem-level $g_s$ slopes during drought). The opposite response between sugar maple and oaks in their stem water withdrawal depending on the soil water availability was similar to the results reported in Matheny et al. (2015), which showed positive correlation between soil water potential and amount of daily withdrawal (i.e., higher withdrawal with higher soil moisture) for sugar maple, while negative correlation (i.e., higher withdrawal with lower soil moisture) was found for oaks, although this pattern was found within a smaller range of soil water potential ($-1.5 < \Psi_S \leq -0.2$) than our range ($-2.20 < \Psi_S \leq -0.05$). We expected tulip poplar to show a similar withdrawal pattern to sugar maple since both of them show more isohydric behaviors than oaks, but tulip poplar increased the withdrawal during the drought period more than sugar maple did (Figure 4). We believe that this is largely due to the fact that withdrawal of stored water is not only dependent on the leaf-level hydraulic regulation or soil water availability but also on the amount of a tree's water storage (Matheny et al. 2015), which would be closely related to the wood traits and tree size rather than leaf-level regulation (Goldstein et al. 1998, Phillips et al. 2003). In our case, the DBH of tulip poplar (62.7–62.8 cm) was ~50% larger than that of sugar maple (41.2–43.8 cm). Further studies about internal water-use dynamics, including applications of frequency domain reflectometry (Hao et al. 2013, Matheny et al. 2015, Oliva Carrasco et al. 2015) and magnetic resonance imaging (Windt et al. 2006, Windt and Blümler 2015), would help to decouple the leaf- and stem-level hydraulic regulations and their response to the changing moisture condition.

### *Dynamics of radial profile of sap flux*

The bell-curve shaped diurnal sap flux pattern observed here was expected (Figure 2), due to the variation of water potential gradient exerted between soil and leaf over a day, and is also consistent with other studies (Granier 1987, Phillips et al. 1996, Burgess et al. 2001, Nadezhdina et al. 2002, Green et al. 2003, Dragoni et al. 2009, Steppe et al. 2010). Oaks showed relatively low sap flux compared with the other species, which was consistent with some previous results (Wullschleger et al. 2001, Pataki and Oren 2003, Bovard et al. 2005), but see Oishi et al. (2008). Our focus in this study, however, was not on the absolute magnitude of sap flux within species but its variation depending on the environmental condition, which is consistent within species and across levels (i.e., leaf and tree; see Figures 2 and 3).

The shift of the radial profile depended on water availability, confirming Hypothesis 1 (Figure 2). Increased water use from inner xylem or even from the outermost layer of heartwood under water limitation has also been reported in previous research (Phillips et al. 1996, Cermak and Nadezhdina 1998, Ford et al. 2004*a*, Kubota et al. 2005, Dragoni et al. 2009, Matheny et al. 2015), although the reason for the shift has not been clearly identified. As a potential explanation, Dragoni et al. (2009) suggested that the substantial changes in tree morphology or phenology caused by prolonged or severe drought would alter the xylem structure and function, eventually affecting the shape of the radial profile of sap flux. Ford et al. (2004*b*) had further hypothesized that increased water potential gradient during periods of high transpiration acts as a driving force to pull the water from the inner sapwood, despite its high hydraulic resistance.

Comparison of multiple radial profile integration methods suggested not only the importance of continuous long-term measurement (i.e., SI vs DI), but also the necessity of considering the variation of sap flux over the sapwood area (i.e., NI vs DI; Table 1). As we demonstrated here, integrating sap flux measurements from a single depth over the entire sapwood area, which is a common approach (Fiora and Cescatti 2006, Ford et al. 2007, Van de Wal et al. 2015), can lead to substantial over- or underestimation of tree water uptake depending on drought status. Applying a variable radial profile is important especially in assessing the impact of environmental changes on tree physiology, as both non-integrated and static sap flux could potentially overrate the impact of drought on the decrease in water flux for all species (Table 1).

Finally, we acknowledge that not only inter-specific but also intra-specific variability of hydraulic traits can be substantial (Anderegg 2015). To minimize intra-specific variability caused by environmental condition, we carefully selected trees with similar DBH that were growing near each other. Despite the fact that within-species variability was overall small in our dataset (Figure 2), the limited number of individuals sampled in this study prevents us from quantifying the inter-specific variability of hydraulic functioning.

## Conclusions

Here, we used leaf-, tree- and stand-level measurements in order to characterize the water-use strategies of common Eastern USA tree species during the severe drought event in 2012, which reduced growing season NEE by more than 50% relative to baseline (1999–2010) mean NEE (Figure 1). Both tree- and leaf-level measurements confirmed the isohydric behavior of sugar maple and tulip poplar, and the anisohydric behavior of oaks (Figure 3). Therefore, we conclude that the sap flux measurements were good proxies for leaf-level gas exchange measurements. As expected, the $g_s$ of isohydric species

declined more significantly during drought as compared with the anisohydric species, with consistent patterns detected in both tree- and leaf-level measurements (Figure 3). Furthermore, comparison of tree- and stand-level measurements enabled us to find evidence of nighttime refilling of trees' water storage, which is considered to be an important mechanism to prevent hydraulic failure (Daley and Phillips 2006, Wang et al. 2012), and in particular to observe a higher reliance of anisohydric oak species on the nighttime refilling (Figure 5). All of these results highlight that isohydric and anisohydric strategies, which are typically used to characterize leaf-level dynamics, are associated with coordinated stem-level behavior. We conclude that the anisohydric species, such as oaks, growing in the mesic Eastern USA would have advantages in their growth under water-limiting conditions, due to their ability to maintain relatively high gas exchange rates via open stomata and higher reliance on the hydraulic capacitance to avoid hydraulic failure. Considering drought-induced mortality is relatively rare in the mesic Eastern USA (Dietze and Moorcroft 2011), this strategy will improve the benefit–risk tradeoff for anisohydric trees (Roman et al. 2015). This can be of particular concern considering the shift in species composition that many Eastern and Midwestern USA forests are experiencing, with an increase in the proportion of shade-tolerant species, such as sugar maple, relative to the shade-intolerant and fire-dependent species, such as oaks (Abrams 2003). These results highlight the impact of changes in species composition on the C and water cycle in the forests under the predicted climate change regime, which will likely promote more severe and frequent drought events in the future (Nepstad et al. 2002, Schär et al. 2004, Salinger 2005, Bréda et al. 2006).

## Acknowledgments

The authors acknowledge support from the National Science Foundation, Division of Environmental Biology, through grant DEB 1552747. We would like to acknowledge the contributions of HaPe Schmid, Sue Grimmond, J.C. Randolph, Steve Scott and the MMSF field crew to the establishment and operation of the MMSF Ameriflux site. We thank the Indiana Department of Natural Resources for supporting and hosting the MMSF AmeriFlux site, and the US Department of Energy, through the Terrestrial Ecosystem Science Program and the AmeriFlux Management Project through the Lawrence Berkeley National Lab, for funding the project. Special thanks to Chris Oishi for valuable comments on nighttime sap flux, and Whitney Moore, Rob Conover, Bo Stearman, Brenten Reust and Ning Zhang for their help in data collection and processing.

## Conflict of interest

None declared.

## References

Abrams MD (1990) Adaptations and responses to drought in *Quercus* species of North America. Tree Physiol 7:227–238.

Abrams MD (2003) Where has all the white oak gone? Bioscience 53: 927–939.

Anderegg WRL (2015) Spatial and temporal variation in plant hydraulic traits and their relevance for climate change impacts on vegetation. New Phytol 205:1008–1014.

Baldocchi D (2008) 'Breathing' of the terrestrial biosphere: lessons learned from a global network of carbon dioxide flux measurement systems. Aust J Bot 56:1–26.

Bellassen V, Luyssaert S (2014) Carbon sequestration: managing forests in uncertain times. Nature 506:153–155.

Binkley D, Burnham H, Allen HL (1999) Water quality impacts of forest fertilization with nitrogen and phosphorus. For Ecol Manage 121: 191–213.

Bonan GB (2008) Forests and climate change: forcings, feedbacks, and the climate benefits of forests. Science 320:1444–1449.

Bovard BD, Curtis PS, Vogel CS, Su HB, Schmid HP (2005) Environmental controls on sap flow in a northern hardwood forest. Tree Physiol 25: 31–38.

Bréda N, Huc R, Granier A, Dreyer E (2006) Temperate forest trees and stands under severe drought: a review of ecophysiological responses, adaptation processes and long-term consequences. Ann For Sci 63: 625–644.

Brzostek ER, Dragoni D, Schmid HP, Rahman AF, Sims D, Wayson CA, Johnson DJ, Phillips RP (2014) Chronic water stress reduces tree growth and the carbon sink of deciduous hardwood forests. Glob Chang Biol 20:2531–2539.

Burgess SSO, Adams MA, Turner NC, Beverly CR, Ong CK, Khan AAH, Bleby TM (2001) An improved heat pulse method to measure low and reverse rates of sap flow in woody plants. Tree Physiol 21: 589–598.

Caspari HW, Green SR, Edwards WRN (1993) Transpiration of well-watered and water-stressed Asian pear trees as determined by lysimetry, heat-pulse, and estimated by a Penman-Monteith model. Agric Forest Meteorol 67:13–27.

Caylor KK, Dragoni D (2009) Decoupling structural and environmental determinants of sap velocity: Part I. Methodological development. Agr For Meteorol 149:559–569.

Cermak J, Nadezhdina N (1998) Sapwood as the scaling parameter – defining according to xylem water content or radial pattern of sap flow? Ann Sci Forest 55:509–521.

Choat B, Jansen S, Brodribb TJ et al. (2012) Global convergence in the vulnerability of forests to drought. Nature 491:752–755.

Ciais P, Reichstein M, Viovy N et al. (2005) Europe-wide reduction in primary productivity caused by the heat and drought in 2003. Nature 437:529–533.

Clearwater MJ, Meinzer FC, Andrade JL, Goldstein G, Holbrook NM (1999) Potential errors in measurement of nonuniform sap flow using heat dissipation probes. Tree Physiol 19:681–687.

Daley MJ, Phillips NG (2006) Interspecific variation in nighttime transpiration and stomatal conductance in a mixed New England deciduous forest. Tree Physiol 26:411–419.

Delzon S, Sartore M, Granier A, Loustau D (2004) Radial profiles of sap flow with increasing tree size in maritime pine. Tree Physiol 24:1285–1293.

Dietze MC, Moorcroft PR (2011) Tree mortality in the eastern and central United States: patterns and drivers. Glob Chang Biol 17: 3312–3326.

Domec JC, Johnson DM (2012) Does homeostasis or disturbance of homeostasis in minimum leaf water potential explain the isohydric versus anisohydric behavior of *Vitis vinifera* L. cultivars? Tree Physiol 32: 245–248.

Dragoni D, Caylor KK, Schmid HP (2009) Decoupling structural and environmental determinants of sap velocity Part II. Observational application. Agric For Meteorol 149:570–581.

Dragoni D, Schmid HP, Wayson CA, Potter H, Grimmond CSB, Randolph JC (2011) Evidence of increased net ecosystem productivity associated with a longer vegetated season in a deciduous forest in south-central Indiana, USA. Glob Chang Biol 17:886–897.

Fiora A, Cescatti A (2006) Diurnal and seasonal variability in radial distribution of sap flux density: implications for estimating stand transpiration. Tree Physiol 26:1217–1225.

Fisher JB, Baldocchi DD, Misson L, Dawson TE, Goldstein AH (2007) What the towers don't see at night: nocturnal sap flow in trees and shrubs at two AmeriFlux sites in California. Tree Physiol 27:597–610.

Flatley WT, Lafon CW, Grissino-Mayer HD, LaForest LB (2013) Fire history, related to climate and land use in three southern Appalachian landscapes in the eastern United States. Ecol Appl 23:1250–1266.

Ford CR, Goranson CE, Mitchell RJ, Will RE, Teskey RO (2004*a*) Diurnal and seasonal variability in the radial distribution of sap flow: predicting total stem flow in *Pinus taeda* trees. Tree Physiol 24:951–960.

Ford CR, McGuire MA, Mitchell RJ, Teskey RO (2004*b*) Assessing variation in the radial profile of sap flux density in *Pinus* species and its effect on daily water use. Tree Physiol 24:241–249.

Ford CR, Hubbard RM, Kloeppel BD, Vose JM (2007) A comparison of sap flux-based evapotranspiration estimates with catchment-scale water balance. Agric For Meteorol 145:176–185.

Ford CR, Laseter SH, Swank WT, Vose JM (2011) Can forest management be used to sustain water-based ecosystem services in the face of climate change? Ecol Appl 21:2049–2067.

Franks PJ, Drake PL, Froend RH (2007) Anisohydric but isohydrodynamic: seasonally constant plant water potential gradient explained by a stomatal control mechanism incorporating variable plant hydraulic conductance. Plant Cell Environ 30:19–30.

Goldammer JG (1999) Ecology – forests on fire. Science 284:1782–1783.

Goldstein G, Andrade JL, Meinzer FC, Holbrook NM, Cavelier J, Jackson P, Celis A (1998) Stem water storage and diurnal patterns of water use in tropical forest canopy trees. Plant Cell Environ 21:397–406.

Granier A (1987) Evaluation of transpiration in a Douglas-fir stand by means of sap flow measurements. Tree Physiol 3:309–319.

Green S, Clothier B, Jardine B (2003) Theory and practical application of heat pulse to measure sap flow. Agron J 95:1371–1379.

Hao G-Y, Wheeler JK, Holbrook NM, Goldstein G (2013) Investigating xylem embolism formation, refilling and water storage in tree trunks using frequency domain reflectometry. J Exp Bot 64:2321–2332.

Hatton TJ, Catchpole EA, Vertessy RA (1990) Integration of sapflow velocity to estimate plant water use. Tree Physiol 6:201–209.

James SA, Clearwater MJ, Meinzer FC, Goldstein G (2002) Heat dissipation sensors of variable length for the measurement of sap flow in trees with deep sapwood. Tree Physiol 22:277–283.

Jones HG (1999) Use of thermography for quantitative studies of spatial and temporal variation of stomatal conductance over leaf surfaces. Plant Cell Environ 22:1043–1055.

Katul GG, Palmroth S, Oren R (2009) Leaf stomatal responses to vapour pressure deficit under current and $CO_2$-enriched atmosphere explained by the economics of gas exchange. Plant Cell Environ 32: 968–979.

Klein T (2014) The variability of stomatal sensitivity to leaf water potential across tree species indicates a continuum between isohydric and anisohydric behaviours. Funct Ecol 28:1313–1320.

Köcher P, Horna V, Leuschner C (2013) Stem water storage in five coexisting temperate broad-leaved tree species: significance, temporal dynamics and dependence on tree functional traits. Tree Physiol 33: 817–832.

Kubota M, Tenhunen J, Zimmermann R, Schmidt M, Adiku S, Kakubari Y (2005) Influences of environmental factors on the radial profile of sap flux density in *Fagus crenata* growing at different elevations in the Naeba Mountains, Japan. Tree Physiol 25:545–556.

Manzoni S, Vico G, Katul G, Palmroth S, Jackson RB, Porporato A (2013) Hydraulic limits on maximum plant transpiration and the emergence of the safety-efficiency trade-off. New Phytol 198:169–178.

Martínez-Vilalta J, Poyatos R, Aguadé D, Retana J, Mencuccini M (2014) A new look at water transport regulation in plants. New Phytol 204: 105–115.

Matheny AM, Bohrer G, Garrity SR, Morin TH, Howard CJ, Vogel CS (2015) Observations of stem water storage in trees of opposing hydraulic strategies. Ecosphere 6:1–13.

McCulloh KA, Johnson DM, Meinzer FC, Woodruff DR (2014) The dynamic pipeline: hydraulic capacitance and xylem hydraulic safety in four tall conifer species. Plant Cell Environ 37:1171–1183.

McDowell N, Pockman WT, Allen CD et al. (2008) Mechanisms of plant survival and mortality during drought: why do some plants survive while others succumb to drought? New Phytol 178:719–739.

Meinzer FC, Johnson DM, Lachenbruch B, McCulloh KA, Woodruff DR (2009) Xylem hydraulic safety margins in woody plants: coordination of stomatal control of xylem tension with hydraulic capacitance. Funct Ecol 23:922–930.

Meinzer FC, Woodruff DR, Eissenstat DM, Lin HS, Adams TS, McCulloh KA (2013) Above- and belowground controls on water use by trees of different wood types in an eastern US deciduous forest. Tree Physiol 33:345–356.

Meir P, Grace J (2005) The response to drought by tropical rain forest ecosystems. In: Malhi Y, Philip OL (eds) Tropical forests and global atmospheric change. Oxford University Press, Oxford, pp 75–86.

Nadezhdina N, Čermák J, Ceulemans R (2002) Radial patterns of sap flow in woody stems of dominant and understory species: scaling errors associated with positioning of sensors. Tree Physiol 22:907–918.

Nadezhdina N, Nadezhdin V, Ferreira MI, Pitacco A (2007) Variability with xylem depth in sap flow in trunks and branches of mature olive trees. Tree Physiol 27:105–113.

Neary DG, Ice GG, Jackson CR (2009) Linkages between forest soils and water quality and quantity. For Ecol Manage 258:2269–2281.

Nepstad DC, Veríssimo A, Alencar A et al. (1999) Large-scale impoverishment of Amazonian forests by logging and fire. Nature 398:505–508.

Nepstad DC, Moutinho P, Dias-Filho MB et al. (2002) The effects of partial throughfall exclusion on canopy processes, aboveground production, and biogeochemistry of an Amazon forest. J Geophys Res Atmos 107: doi: 10.1029/2001JD000360.

Novick KA, Oren R, Stoy PC, Siqueira MBS, Katul GG (2009) Nocturnal evapotranspiration in eddy-covariance records from three co-located ecosystems in the Southeastern U.S.: implications for annual fluxes. Agric For Meteorol 149:1491–1504.

Novick KA, Oishi AC, Ward EJ, Siqueira MBS, Juang JY, Stoy PC (2015) On the difference in the net ecosystem exchange of $CO_2$ between deciduous and evergreen forests in the southeastern United States. Glob Chang Biol 21:827–842.

Novick KA, Miniat CF, Vose JM (2016) Drought limitations to leaf-level gas exchange: results from a model linking stomatal optimization and cohesion-tension theory. Plant Cell Environ 39:583–596.

Oishi AC, Oren R, Stoy PC (2008) Estimating components of forest evapotranspiration: a footprint approach for scaling sap flux measurements. Agric For Meteorol 148:1719–1732.

Oliva Carrasco L, Bucci SJ, Di Francescantonio D et al. (2015) Water storage dynamics in the main stem of subtropical tree species differing in wood density, growth rate and life history traits. Tree Physiol 35: 354–365.

Oren R, Sperry JS, Katul GG, Pataki DE, Ewers BE, Phillips N, Schäfer KVR (1999) Survey and synthesis of intra- and interspecific variation in stomatal sensitivity to vapour pressure deficit. Plant Cell Environ 22: 1515–1526.

Pataki DE, Oren R (2003) Species differences in stomatal control of water loss at the canopy scale in a mature bottomland deciduous forest. Adv Water Resour 26:1267–1278.

Phillips N, Oren R, Zimmermann R (1996) Radial patterns of xylem sap flow in non-, diffuse- and ring-porous tree species. Plant Cell Environ 19:983–990.

Phillips N, Oren R, Zimmermann R, Wright SJ (1999) Temporal patterns of water flux in trees and lianas in a Panamanian moist forest. Trees Struct Funct 14:116–123.

Phillips NG, Ryan MG, Bond BJ, McDowell NG, Hinckley TM, Čermák J (2003) Reliance on stored water increases with tree size in three species in the Pacific Northwest. Tree Physiol 23:237–245.

Regalado CM, Ritter A (2007) An alternative method to estimate zero flow temperature differences for Granier's thermal dissipation technique. Tree Physiol 27:1093–1102.

Roman DT, Novick KA, Brzostek ER, Dragoni D, Rahman F, Phillips RP (2015) The role of isohydric and anisohydric species in determining ecosystem-scale response to severe drought. Oecologia 179:641–654.

Salinger M (2005) Increasing climate variability and change: reducing the vulnerability. Clim Change 70:1–3.

Schär C, Vidale PL, Lüthi D, Frei C, Häberli C, Liniger MA, Appenzeller C (2004) The role of increasing temperature variability in European summer heatwaves. Nature 427:332–336.

Schmid HP, Grimmond CSB, Cropley F, Offerle B, Su HB (2000) Measurements of $CO_2$ and energy fluxes over a mixed hardwood forest in the mid-western United States. Agric For Meteorol 103: 357–374.

Scholz FG, Phillips NG, Bucci SJ, Meinzer FC, Goldstein G (2011) Hydraulic capacitance: biophysics and functional significance of internal water sources in relation to tree size. In: Meinzer FC, Lachenbruch B, Dawson TE (eds) Size- and age-related changes in tree structure and fuction. Springer, Dordrecht, pp 341–361.

Schwenk WS, Donovan TM, Keeton WS, Nunery JS (2012) Carbon storage, timber production, and biodiversity: comparing ecosystem services with multi-criteria decision analysis. Ecol Appl 22:1612–1627.

Shinohara Y, Tsuruta K, Ogura A, Noto F, Komatsu H, Otsuki K, Maruyama T (2013) Azimuthal and radial variations in sap flux density and effects on stand-scale transpiration estimates in a Japanese cedar forest. Tree Physiol 33:550–558.

Steppe K, De Pauw DJW, Doody TM, Teskey RO (2010) A comparison of sap flux density using thermal dissipation, heat pulse velocity and heat field deformation methods. Agric For Meteorol 150:1046–1056.

Swanson RH, Whitfield DWA (1981) A numerical analysis of heat pulse velocity theory and practice. J Exp Bot 32:221–239.

Thomsen JE, Bohrer G, Matheny AM, Ivanov VY, He LL, Renninger HJ, Schafer KVR (2013) Contrasting hydraulic strategies during dry soil conditions in *Quercus rubra* and *Acer rubrum* in a sandy site in Michigan. Forests 4:1106–1120.

Tyree MT, Sperry JS (1988) Do woody plants operate near the point of catastrophic xylem dysfunction caused by dynamic water stress?: answers from a model. Plant Physiol 88:574–580.

Van de Wal BAE, Guyot A, Lovelock CE, Lockington DA, Steppe K (2015) Influence of temporospatial variation in sap flux density on estimates of whole-tree water use in *Avicennia marina*. Trees Struct Funct 29:215–222.

Verbeeck H, Steppe K, Nadezhdina N et al. (2007) Model analysis of the effects of atmospheric drivers on storage water use in Scots pine. Biogeosciences 4:657–671.

Verkerk PJ, Levers C, Kuemmerle T, Lindner M, Valbuena R, Verburg PH, Zudin S (2015) Mapping wood production in European forests. For Ecol Manage 357:228–238.

Wang H, Zhao P, Hölscher D, Wang Q, Lu P, Cai XA, Zeng XP (2012) Nighttime sap flow of *Acacia mangium* and its implications for nighttime transpiration and stem water storage. J Plant Ecol 5:294–304.

Wayson CA, Randolph JC, Hanson PJ, Grimmond CSB, Schmid HP (2006) Comparison of soil respiration methods in a mid-latitude deciduous forest. Biogeochemistry 80:173–189.

Wear DN, Greis JG (2012) The southern forest futures project: summary report. Gen. Tech. Rep. SRS-GTR-168. USDA-Forest Service, Southern Research Station, Asheville, NC, 54 p.

Windt CW, Blümler P (2015) A portable NMR sensor to measure dynamic changes in the amount of water in living stems or fruit and its potential to measure sap flow. Tree Physiol 35:366–375.

Windt CW, Vergeldt FJ, de Jager PA, van As H (2006) MRI of long-distance water transport: a comparison of the phloem and xylem flow characteristics and dynamics in poplar, castor bean, tomato and tobacco. Plant Cell Environ 29:1715–1729.

Wullschleger SD, King AW (2000) Radial variation in sap velocity as a function of stem diameter and sapwood thickness in yellow-poplar trees. Tree Physiol 20:511–518.

Wullschleger SD, Meinzer FC, Vertessy RA (1998) A review of whole-plant water use studies in trees. Tree Physiol 18:499–512.

Wullschleger SD, Hanson PJ, Todd DE (2001) Transpiration from a multi-species deciduous forest as estimated by xylem sap flow techniques. For Ecol Manage 143:205–213.

Xiao J, Zhuang Q, Law BE et al. (2011) Assessing net ecosystem carbon exchange of U.S. terrestrial ecosystems by integrating eddy covariance flux measurements and satellite observations. Agric For Meteorol 151: 60–69.

Zang D, Beadle CL, White DA (1996) Variation of sapflow velocity in *Eucalyptus globulus* with position in sapwood and use of a correction coefficient. Tree Physiol 16:697–703.